

# RSC Advances



This is an *Accepted Manuscript*, which has been through the Royal Society of Chemistry peer review process and has been accepted for publication.

*Accepted Manuscripts* are published online shortly after acceptance, before technical editing, formatting and proof reading. Using this free service, authors can make their results available to the community, in citable form, before we publish the edited article. This *Accepted Manuscript* will be replaced by the edited, formatted and paginated article as soon as this is available.

You can find more information about *Accepted Manuscripts* in the [Information for Authors](#).

Please note that technical editing may introduce minor changes to the text and/or graphics, which may alter content. The journal's standard [Terms & Conditions](#) and the [Ethical guidelines](#) still apply. In no event shall the Royal Society of Chemistry be held responsible for any errors or omissions in this *Accepted Manuscript* or any consequences arising from the use of any information it contains.

# Curcumin Associated Poly (Allylamine Hydrochloride)-Phosphate Self-Assembled Hierarchically Ordered Nanocapsules: Size Dependent Investigation on Release and DPPH Scavenging Activity of Curcumin

Mai Mouslmani<sup>1</sup>, Jessica M. Rosenholm<sup>2</sup>, Neeraj Prabhakar<sup>2</sup>, Markus Peurla<sup>3</sup>, Elias Baydoun<sup>4</sup>  
Digambara Patra<sup>1\*</sup>

<sup>1</sup>Department of Chemistry, American University of Beirut, Beirut, Lebanon,  
Email: [dp03@aub.edu.lb](mailto:dp03@aub.edu.lb)

<sup>2</sup>Laboratory for Physical Chemistry, Åbo Akademi University, Turku, Finland;

<sup>3</sup>Laboratory of Electron Microscopy, University of Turku, Turku, Finland;

<sup>4</sup>Department of Biology, American University of Beirut, Beirut, Lebanon;

**Keywords:** PAH, Curcumin, Phosphate, Silica Nanoparticles, Nanocapsules.

---

\*Corresponding Author Email: [dp03@aub.edu.lb](mailto:dp03@aub.edu.lb)

Tel: +9611350 000 ext 3985; Fax: +9611365217(DP)

## Abstract

Combination of a cationic polyamine with a multivalent anionic salt results in the spontaneous generation of ionically crosslinked capsules. Here we report curcumin associated poly (allylamine hydrochloride) crosslinks with dipotassium phosphate and subsequently congregates with silica nanoparticles to form hierarchically ordered nanocapsule structures. The capsule sizes vary depending on the concentration of dipotassium phosphate. SEM data ascertain spherical shape of the nanocapsules and TEM analysis demonstrates that the outer layer made up of silica has a thickness of ~50–250 nm. The fluorescence images confirm that curcumin are present all over the capsules. Strong interaction between nanocapsules and curcumin is evident from spectroscopic analysis and TGA data. Release of curcumin from the nanocapsules is found to be triggered by pH where basic environment trigger the maximum release compared to acidic and neutral conditions. The drug release profile of curcumin from the nanocapsules follows the Higuchi model and depends on the size of the nanocapsules. 2,2-diphenyl-1-picrylhydrazyl (DPPH) scavenging activity of the encapsulated curcumin decreases exponentially with a decrease in size of the nanocapsules, suggesting not only weight percentage of curcumin in the nanocapsules plays a role but also availability of  $\beta$ -diketone group of curcumin for H-donation is vital. Thus, in larger nanocapsules more curcumin per surface area of the nanocapsules are exposed on the outside for scavenging activity, compared to smaller sized nanocapsules where a substantial percentage of curucmin are buried/encapsulated inside the capsules without exposing themselves for scavenging activity.

## 1. Introduction

At present, material chemists widely use hard and soft-templating synthesis methods for capsule structure preparations. However, drawbacks related to long synthetic steps and high cost, have limited their use in practical applications<sup>1</sup>. To solve these difficulties, a relatively new concept of capsule formation via polyamine-salt aggregate or 'PSA' has been developed<sup>2,3</sup>. This technique was originally termed as 'tandem self-assembly' (see **Figure 1** ). It involves combination of a cationic polyamine with a multivalent anionic salt, resulting in the spontaneous generation of ionically crosslinked PSAs<sup>4,5</sup>. The capsule is formed through further addition of negatively charged shell material on PSAs that serves as the capsule template<sup>6,7</sup>. For further use, the polyamine-salt template can remain in the capsule's core; however, after shell formation it can spontaneously disassemble, depending on polymer and salt types, leaving a capsule with a water filled core. As the polymer part participates in shell formation and is a main shell constituent, the PSA is not strictly a soft or hard templating method<sup>8</sup>.

Curcumin, bis (4- hydroxy -3- methoxyphenyl) -1, 6- diene- 3, 5- dione<sup>9</sup>, is a natural diphenolic yellow orange pigment extracted from the dried rhizome of turmeric *Curcuma longa*, a perennial herb that is widely cultivated in southeast and south tropical Asia<sup>10</sup>. Chemically curcumin (CU) is a  $\beta$ - diketone that tautomerizes between its enol and keto structures (see **Scheme 1**). The diketo form is favoured in solid phase of CU, while enol form in solution<sup>11</sup>. CU is a major component of curry spice, and it is extensively used in traditional Arabic and Indian cooking. For industrial applications, CU is used as a dye for the conservation and colouring of food, as well in cosmetics. Concerning its therapeutic efficiency, CU has been applied as a house-hold drug since the ancient times<sup>12,13</sup>, where its anti- inflammatory and healing properties are even reported in the books of *ayurveda*. In the last 20 years, a large number of publications have shown that CU

depicts effective therapeutic properties not only as an anti-inflammatory drug<sup>14</sup>, but also as a chemo-preventive<sup>15,16</sup>, chemotherapeutic<sup>17,18</sup>, anti-oxidant<sup>15,19</sup>, anti-amyloid<sup>20</sup>, antiarthritic<sup>21</sup>, anti-HIV<sup>22</sup>, hepatoprotective<sup>20</sup>, antimicrobial<sup>23,24</sup> and thrombosuppressive<sup>25</sup> agent. In addition, CU is being used in the treatment of cystic fibrosis<sup>26</sup> and Alzheimer disease<sup>27</sup>. Research over the last few decades has proven that CU owes a strong therapeutic potential against numerous types of cancer. CU has been shown to inhibit the proliferation, metastasis and transformation of tumours; where it has been demonstrated that it arrests the cancer cells in various phases of the cell cycle and induces apoptosis (programmed cell death)<sup>10</sup>.

Although CU has numerous medicinal benefits with high safety profiles, even at doses as high as 8 g day<sup>-1</sup>, the administration of CU to patients has a serious practical limitation<sup>28</sup>. Wahlstrom et al.<sup>29</sup> reported that when rats were administered CU at a dose 1 g/Kg, about 3/4th of CU was excreted in the feces, whereas negligible amounts of CU were present in the urine. Blood plasma levels and biliary excretions measurements showed that CU is poorly absorbed in the gut; moreover, the CU's quantity that reaches tissues outside the gut is pharmacologically insignificant. Hence, to reach the therapeutic effects of CU in the human body, a person must ingest between 12 to 20 g of CU daily<sup>30</sup>. The low bioavailability and poor water solubility (i.e. 0.0004 mg ml<sup>-1</sup> at pH 7.3) of CU can be solved by applying nanotechnological delivery approaches<sup>31</sup>. CU has been encapsulated in bovine serum albumin, chitosan<sup>32</sup>, liposomes<sup>33</sup>, polymeric nanoparticles and silica particles<sup>34-39</sup>. It has also been complexed with phospholipids and cyclodextrin<sup>33</sup>. The synthesis of curcumin- encapsulated polymeric nanoparticles of N-isopropylacrylamide with N- vinyl-2- pyrrolidone and poly (ethyleneglycol)monoacrylate has recently been reported<sup>30</sup>. CU has been encapsulated in poly (<sub>L</sub>-lysine) termed as Micro-curcumin<sup>40</sup>. The later approach is based on polymer block self-assembly on the surfaces of

nanoparticles using citrate salt. The formed microcapsules are spherical with a core/shell structure<sup>41,42</sup>. Zhang et al have recently adopted this procedure<sup>2,40-42</sup> by replacing poly (L-lysine) with poly (allylamine hydrochloride) and using two fluorescence markers for pH sensing<sup>43</sup>. These capsules are hollow and large. We have also found that excited state intra-molecular hydrogen transfer could be revoked depending on the size of the nanocapsules using (allylamine hydrochloride) (PAH)<sup>44</sup>. However, these nanocapsules were found not to be hollow. In the present study, we prepared and investigated PAH nanocapsules for the release of curcumin in different pH. The aim is to encapsulate CU in PAH (see **Scheme 2**) based nanocapsules; where CU associated PAH crosslink with dipotassium phosphate and consequently congregates SiO<sub>2</sub> nanoparticles to form hierarchically ordered nanocapsule (NC) structures of 100-1000 nm size depending on the concentration of dipotassium phosphate. The advantages of the present method are: (i) the ease of preparation and purification of the nanocapsules; (ii) unlike earlier delivery systems with silica particles, the formation of template is in situ, hence no need for a performed template and polymerization/ hydrolysis under acidic condition; (iii) finally, it is fast and doesn't require long hours of preparation steps.

## **2. Materials and Methods:**

### *2.1 Materials*

CU was obtained from Acros Organics and directly used without further purification. CU is poorly soluble in water and degrades in aqueous medium, so the stock solution of CU was prepared in 10 % acetone/ de-ionized water. Poly(allylamine hydrochloride) and Silica LUDOX<sup>®</sup> HS-40 Colloidal Silica, 40 wt% suspension in water, were obtained from Sigma- Aldrich. PAH stock solution was prepared in de-ionized water of pH 4.4 to ensure the formation of

PAH/dipotassium phosphate aggregates. Dipotassium phosphate used was obtained from SOLAR LABORATORIES and its stock solution was prepared in de-ionized water.

### *2.2 Preparation of nanocapsules*

Nanocapsules were prepared by mixing 1.3 ml of 3 mg ml<sup>-1</sup> poly (allylamine hydrochloride), PAH (pKa = 8.6), with 0.5 ml of 1 mg ml<sup>-1</sup> of CU. Then, self-assembly of the mixture solution was achieved by cross-linking the CU-PAH chains with 7.8 ml of 2.5 mM dipotassium phosphate in aqueous media at pH 4.4 and aged for 30 minutes. Afterwards, 7.8 ml of 40 wt. % suspension of silica nanoparticles (SiO<sub>2</sub> NPs) at pH ~ 9.8 was added to this aggregated solution. The cloudy solution was kept for 2 hours, and then centrifuged at a speed of 4450 rpm for 20 minutes. The NCs formed were washed 3 times in de-ionized water. For preparation of different size nanocapsules, concentration of dipotassium phosphate was varied accordingly, for example, 3.14 mM of dipotassium phosphate used for NC1; 1.8 mM for NC2; 960 μM for NC3 and 10 μM for NC4.

### *2.3 Morphological Characterization*

Scanning electron microscopy (SEM) analysis was done using Tescan, Vega 3 LMU with Oxford Edx detector (Inca XmaW20) SEM, where 3 mg of the NC were dissolved in 5 ml of de-ionized water, and few drops of the nanocapsule suspension were mounted on an aluminium stub, coated with carbon adhesive. After being dried the sample was ready for the SEM analyses. Transmission electron microscopy (TEM) measurement was carried out with a JEOL JEM-1400Plus, operating at 120 kV. TEM samples were prepared by casting a drop of the nanoparticle suspension onto copper grids covered with carbon films. The fluorescence image was recorded using a high sensitive STED confocal set up consisted of confocal microscope (Leica TCS SP5 STED, Leica Microsystem), an Argon laser with 430 nm excitation wavelength and APD

detector. CU was excited by a wavelength of 430 nm and emission was collected using a band filter in the range of 460 –600 nm. The particle size distribution was analyzed using DLS (Brookhaven Instruments Corps) technique; with a laser source of 658 nm and a PMT detector (HAMAMATSU, HC120-30). The software used was 90Plus Particle Sizing Software Ver. 5.23 and the dust was set at 40.

#### *2.4 Spectroscopic Measurements*

The absorption spectra were recorded using a JASCOV-570 UV-VIS-NIR Spectrophotometer at room temperature. The steady-state fluorescence spectra (excitation and emission) were recorded at room temperature using Jobin-Yvon-Horiba Fluorolog III fluorometer and the FluorEssence program where the excitation and emission slits width were 5 nm. The source of excitation was a 100 W Xenon lamp, and the used detector was R-928 operating at a voltage of 950 V. FT-IR-Raman spectrometer (Thermo-Nicolet, Nexus 870) was used to record the Raman spectra in the range of 4000 to 400  $\text{cm}^{-1}$ .

#### *2.5 Other Measurements*

The apparent zeta potential was measured using a Malvern Zetasizer Nano ZS (M3-PALS) using the Non-Invasive Back Scatter technique. The instrument was equipped with a monochromatic red laser operating at 632.8 nm and the data were analyzed with the Malvern Dispersion technology software. Z-average values for three measurements were recorded. The Thermogravimetric Analysis (TGA) and Differential Scanning Calorimetry (DSC) measurements were done using a Netzsch TGA 209 in the temperature range 0 to 800 °C with an increment of 30 K/ 10 minutes in a N<sub>2</sub> atmosphere.

#### *2.6 Measurement of curcumin release*

The nanocapsules were dissolved in 3 ml of the desired pH solution (5, 7 or 8) and aged for a given interval of time before centrifugation. The samples were centrifuged for 20 minutes at 4450 rpm. The precipitate was left and the solution was collected to measure the absorbance of CU for quantification.

### *2.7 Testing biological activity of curcumin*

The 2,2-diphenyl-1-picrylhydrazyl (DPPH) (see **Scheme 3**) scavenging activity of curcumin could be simply measured by following the change in absorbance of DPPH at 520 nm and biological activity of curcumin embedded in the nanocapsules can be understood. Therefore, we adopted a similar procedure reported earlier<sup>45,46</sup> where curcumin samples were mixed with DPPH in the double distilled de-ionized water. The concentration of DPPH was kept constant throughout the experiment. The changes in absorption of DPPH at 520 nm were recorded at room temperature. Lower in change in the absorbance ( $\Delta A$ ) at 520 nm refers to higher DPPH scavenging activity. Similarly, higher value of  $1/\Delta A$  indicates higher scavenging activity.

## **3. Results and Discussion**

Nanocapsules were prepared by mixing poly (allylamine hydrochloride), ( $pK_a = 8.6$ ), with CU. The interaction of CU with PAH was found to be strong due to electrostatic as well as hydrophobic interaction between them; it has been reported that such interactions play a crucial role in the encapsulation chemistry<sup>2,41</sup>. Then, self-assembly of the mixture solution was achieved by cross-linking the CU-PAH chains with dipotassium phosphate in aqueous media at pH 4.4. It is worth to mention that the ionic-crosslinking of polyamines by anionic salts occurs when both have their respective charge, where the latter depends on the  $pK_a$  values of the salt and polymer<sup>2</sup>. Therefore, a pH of 4.4 maintains the positive and negative charge of PAH ( $pK_a=8.6$ ) and dipotassium phosphate ( $pK_{a1}=2.15$ ,  $pK_{a2}=6.82$  and  $pK_{a3}=12.38$ ) respectively. Afterwards, silica

nanoparticles (SiO<sub>2</sub> NPs) at pH ~ 9.8 was added to this aggregated solution. It should be noted that the pH of the colloidal solution increased to 9.5 while adding silica solution. In this course, it has been reported<sup>2</sup> that the capsule shell formation depends on the isoelectric point (IEP) of the nanoparticle (NP) material, where it determines if the NPs will be negatively charged at the pH of the final solution of the polyamine/salt-NP mixture. Before depositing within the shell region, the shell material diffuses through the outer portion of the polyamine/salt aggregate via charge interaction with the positively charged polyamine. Herein, the final pH (9.5) of our capsule mixture ensures the diffusion and deposition of silica NPs (IEP~3.5) on the surface of PAH/dipotassium phosphate aggregates. Due to their overall net positive charge, these aggregates of CU–PAH–dipotassium phosphate could assist the assembly of negatively charged silica nanoparticles, which then shape into hierarchically ordered nanocapsule structures<sup>41</sup> as illustrated in **Figure 1**.

The SEM images depicted in **Figure 2 (a,b)**, show that the NCs are spherical. The SEM image of the CU–PAH–dipotassium phosphate mixture, before silica nanoparticles were added suggests that smaller size spherical aggregates are formed before the silica nanoparticles are added<sup>44</sup>. The particle size distribution of the nanocapsules was analyzed by a dynamic light scattering (DLS) method, and was found to have an effective hydrodynamic radius ( $R_h$ ) of 480 nm for 2.5 mM of dipotassium phosphate. The TEM image, **Figure 3a&b** of NCs confirms that the silica particles are at the surface. The thickness of the silica layer was about 50–250 nm. The fluorescence image, **Figure 3c&e**, indicates that the fluorescence is originating from all over the capsules, suggesting that CU is homogeneously distributed throughout the capsules. The 3D orientation of Figure 3b (after rotating 180 degrees) is shown in Figure 3c, which further confirms fluorescence is coming from all over the sphere (nanocapsules) rather from one side of the sphere, thus,

curcumin is located all around the spherical nanopcapsules. The fluorescence of curcumin was further established by fluorescence spectroscopic measurements as reported earlier<sup>44</sup>.

PAH has a strong binding affinity with curcumin, which was confirmed by the high value of their association constant ( $K=1.44 \times 10^4 \text{ M}^{-1}$ ). The latter was found by measuring the fluorescence emission spectra of CU at constant concentration ( $3.33 \times 10^{-3} \text{ mg ml}^{-1}$ ) with various PAH (polymer) concentration from 0 to  $3 \text{ mg ml}^{-1}$ ; where the excitation wavelength was 350 nm. The association constant was calculated using the following equation<sup>47</sup>:

$$\text{Log} \left[ \frac{(F-F_0)}{F_0} \right] = \text{Log}(K) + n \text{Log}[PAH]$$

where K and n are the binding constant and the number of binding sites, respectively. F and  $F_0$  are the fluorescence intensity of curcumin at 450 nm in the presence and absence of PAH. Based on the later equation the plot of [PAH] vs.  $(F-F_0)/F_0$  (**Figure 4a**) demonstrated an excellent linear relationship with linear regression  $R^2 = 0.99424$ ,  $n = 0.91$  and  $K = 1.44 \times 10^4 \text{ M}^{-1}$ . This value is similar to association constant obtained for curcumin with albumin<sup>48</sup>.

The apparent zeta potential provides information related to the effective (net) surface charge. Curcumin is known to be found in enolic form in solution. The zeta potential measurement of curcumin in double distilled deionized water (pH 7) showed a value close to  $-40 \text{ mV}$  whereas that of silica NPs used in this study was found to be  $-37 \text{ mV}$  in water. Zeta potential distribution of PAH in water gave a value of  $+7 \text{ mV}$ . When we measure the zeta potential of PAH and curcumin mixture, this value was found to be  $+47 \text{ mV}$ . This value suggests that interaction of PAH and curcumin is electrostatic and association of curcumin with PAH increases the positive surface charge. This latter increase in surface charge can be explained by the interaction of  $\text{N}^+$  of PAH and enol oxygen of curcumin, as also confirmed by the FT-IR spectra later on. On the other hand, when PAH was mixed with  $\text{K}_2\text{HPO}_4$  in the same ratio as the experimental conditions used

for synthesizing nanocapsules, this value was close to zero. This value did not change appreciably for the mixture of  $K_2HPO_4$  and PAH in the presence of curcumin with a zeta potential value close to 0 mV. However, when silica was added and the nanocapsules were formed, the apparent zeta potential value was found to be  $-38$  mV (see **Figure 4b**). This means that our synthesized nanocapsules is similar to that of the pristine silica particles.

The hydrodynamic diameter size distribution was found to be  $0.2\text{--}1$   $\mu\text{m}$ . Increasing the concentration of dipotassium phosphate to 5 mM increased the  $R_h$  value to 610 nm. As depicted in Figure 5a&b, 3.14 mM of dipotassium phosphate gave a  $R_h$  value of 500 nm (designated as NC1); similarly, decreasing the salt concentration to 1.8 mM had a  $R_h$  value of 218 nm (designated as NC2). 960  $\mu\text{M}$  and 10  $\mu\text{M}$  of dipotassium phosphate produced with  $R_h$  of 164 nm (designated as NC3) and 133 nm (designated as NC4), respectively. However, the SEM images show that the NCs were found to be much smaller ( $R_h = \sim 60$  nm) at the low salt concentration. The high effective hydrodynamic radius is due to the further aggregation of smaller size NCs in solution. The initial size of the core depends on the number of PAH chains that are ionically crosslinked by dipotassium phosphate. This, in turn, is dependent on the amount of salt added<sup>2,43</sup>. At low salt concentrations, fewer counter-ions are displaced still keeping PAH rigid with fewer sites to crosslink with other chains. The increase in the concentration of dipotassium phosphate increases the negative charges of the salt per positive charge of PAH, which encourages the formation of larger aggregates, thus, increasing the size of the core as well as the hydrodynamic radius of the NC<sup>2,44</sup>. Such an aggregation was also noticed when NCs were prepared in solution and dried on a carbon adhesive before recording the SEM images. The aggregated form of NCs were also noticed in the fluorescence images (Figure 3c). The absorption spectrum of NCs were found to be similar to that of CU (see Figure S1 (a)), however,

the  $S_0 \rightarrow S_2$  transition of CU at  $\sim 266$  nm was not well resolved in NC. The absorption spectra of NCs did not change in the spectral shape and position for various sizes, however, the change in absorbance could be linked with the amount of curcumin present in the capsules, which was estimated using TGA data as discussed subsequently.

Nanoparticles often possess novel physical and chemical properties. Resonance Rayleigh Scattering (RRS) or surface Plasmon resonance (SPR) are widely used in the field of probes and sensors<sup>49</sup>. The principles behind these phenomena is elastic scattering<sup>50</sup>. RRS is produced when the wavelength of Rayleigh scattering is located at or close to the molecular absorption band. When the analyte interacts with the probe, the intensity of RRS is greatly increased. This is a simple technique and has been used for nanoparticles earlier<sup>51</sup>. RRS can be measured by applying synchronous fluorescence spectroscopy (SFS) by keeping the wavelength interval ( $\Delta\lambda$ ) at 0 nm. The SFS spectra of CU and NCs are shown in Figure S1(b). CU gave a major and broad peak at around  $\sim 550$  nm along with small peaks at  $\sim 280$  nm,  $\sim 370$  nm and  $\sim 450$  nm in the resonance Rayleigh scattering spectrum. Interestingly, the small peak at  $\sim 288$  nm got remarkably enhanced in the NCs ( $> 10$  times). The maximum at  $\sim 288$  nm obtained for NC1 was blue shifted to  $\sim 277$  nm for the smallest sized nanocapsules, NC4 ( $R_h = \sim 60$  nm) but this change in SFS maximum was not remarkable among nanocapsules but was appreciable compared to curcumin alone (see Figure 5c). Subsequently, increase in the size of the NCs reduced the fluorescence intensity marginally by slightly showing a red shift in the maximum (see Figure 5d). Noticeably, the peak at  $\sim 370$  nm in CU was completely abolished in NCs and the CU peak at  $\sim 550$  nm was well resolved in all the NCs. The enhancement of RRS intensity at  $\sim 288$  nm is due to formation of nanocapsules which increases the scattering intensity.

TGA data of raw curcumin indicated that the weight-loss occurs around 260 °C and continues till 550 °C. DSC curve gave a major peak at around 500 °C. However, in the case of nanocapsules, the weight-loss started much earlier at around 120 °C and continued to 550 °C. The early weight loss is due to presence of PAH in the nanocapsules as depicted in **Figure 6a**. Similarly, in DSC curve a sharp peak appeared at 300 °C and the peak at 500 °C found in raw curcumin was found as hump. TGA was further used to estimate percentage of curcumin present in these capsules as shown in **Figure 6b**. It was found that nanocapsules having the largest size had the highest percentage of curcumin, about 7 %, whereas the rest of the capsules showed about 4 % mass loss during thermal degradation that could be related to combustion of CU. However, the concentration of curcumin measured from spectrophotometric measurements gave 6 % of CU in NC1, 3 % for NC2, NC3 and NC4. The ~1% difference in values obtained from both the measurements could be due to degradation of other organic materials along with curcumin and/or due to difference in methodology. Nevertheless, the trend was similar in both the methods and such minor difference in curcumin estimation does not play any significant role during its release.

As shown in **Figure S2**, the observed Raman shift of curcumin at around 3200  $\text{cm}^{-1}$  might be due to an OH band, which is reported to appear at 3545  $\text{cm}^{-1}$  in  $\text{CCl}_3$  and this band downshifted strongly to 3374  $\text{cm}^{-1}$  in acetonitrile<sup>52</sup>. Since aqueous environment heightens the possibilities of hydrogen bonding between curcumin and water (solvent) molecules much more than acetonitrile (solvent), the downshift of OH band is much more expected, thus our observation of 3200  $\text{cm}^{-1}$  in Raman spectra for curcumin in water is not surprising. However, we did not find this peak in the nanocapsules. The obtained Raman spectra at around 3060 and 3010  $\text{cm}^{-1}$  for curcumin are assigned to aromatic C-H<sub>stretching</sub>. These peaks were noticed in nanocapsules. PAH gave a strong

Raman spectrum at around  $2930\text{ cm}^{-1}$  which is assigned to strong aliphatic CH band, this band is also found in the nanocapsules. Absence of peaks in the region of  $1650 - 1800\text{ cm}^{-1}$  in Raman spectra of curcumin further suggest that curcumin largely exists in enol form rather than keto form, hence, corroborating earlier findings. The band at  $1630\text{ cm}^{-1}$  is due to phenolic OH group. These peaks were predominantly present in the nanocapsules. However, the Raman shift at  $1626\text{ cm}^{-1}$  is due to  $\nu_{\text{C}=\text{C}}$  and  $\nu_{\text{C}=\text{O}}$  of curcumin, which is the same as reported experimental value and close to computed values  $1630\text{ cm}^{-1}$  and  $1615\text{ cm}^{-1}$  respectively<sup>52</sup>. The band at  $1601\text{ cm}^{-1}$  and  $1492\text{ cm}^{-1}$  is due to aromatic vibration  $\nu_{\text{C}=\text{Cring}}$  of curcumin. The  $\delta_{\text{CH}_3}$  band at  $1456\text{ cm}^{-1}$ ,  $\delta_{\text{PhCCHOHenol}}$  band at  $1314\text{ cm}^{-1}$  and the band at  $1247\text{ cm}^{-1}$  are due to  $\delta_{\text{COHenol}}$  of curcumin and were present in nanocapsules' spectra. Earlier<sup>44</sup> it is found from FT-IR spectral data that the phenolic O-H vibration of CU was observed at  $\sim 3509\text{ cm}^{-1}$  and  $3400\text{ cm}^{-1}$  whereas the peaks found in the range  $3392 - 3033\text{ cm}^{-1}$  in PAH is associated with the N-H stretch. All these prominent peaks in the control samples were not visible in NCs instead of a major peak found at  $3448\text{ cm}^{-1}$ . Similarly the peak at  $2972\text{ cm}^{-1}$  due to enolic O-H vibration could be detected in CU, but was not clear in NCs. Further, the control peaks at  $1627\text{ cm}^{-1}$  and  $1603\text{ cm}^{-1}$  for CU are associated with the C=O and C=C vibrations. C=O vibration has another peak at  $1510\text{ cm}^{-1}$ . On the other hand for PAH, the peaks at  $1608\text{ cm}^{-1}$  and  $1457\text{ cm}^{-1}$  are associated with the N-H asymmetric bending and C-H bending. In NCs in these regions only a prominent peak was obtained at  $1636\text{ cm}^{-1}$  confirming a strong involvement  $-\text{NH}_2$  of PAH and enol form of CU inside the NCs.

The release of drug from the NCs is very important for their application as drug delivery vehicles. Delivery of curcumin in different environments was investigated by changing the pH of the solution and the degree of CU release from the nanocapsules was estimated by absorption spectrophotometry. It was found that the CU was released from the nanocapsules in acidic

(pH=5.0), basic (pH=8.0) and neutral (pH= 7.0) conditions as shown in **Figure 7a**. However, release of CU was triggered faster in basic environment than acidic (~42% relative to basic environment) and neutral (~20% relative to basic environment).

Furthermore, it was found that there is a linear relationship between the amounts of CU released vs. time studied. An equation was proposed by Higuchi<sup>53</sup> where the rate of drug release is related to physical constants based on simple diffusion laws as  $R=K_H t^{1/2}$  where R is the amount of drug released,  $K_H$  is the Higuchi dissolution constant and t is the time. We applied the equation for CU release from NC1 in different pH environments (see **Figure 7b**) and as expected Higuchi dissolution constant ( $K_H$ ) was found to be 2.5 times higher in basic environment compared to in acidic medium and 8 times higher compared to neutral condition. Many studies have suggested that cancerous cells are acidic; therefore, the release of CU was studied for different nanocapsules in acidic environment (see **Figure 8a**). Moreover, it was found that the Higuchi dissolution constant is related to the particle size, where it increases exponentially with the increase in the NCs hydrodynamic radius ( $R_h$ ) (see **Figure 8b**).

Apart from drug delivery, biological activity of the drug molecule within the delivery system has immense importance. **Figure 9** gives the values of absorbance of DPPH at 520 nm in the presence of 0.5 mg/mL curcumin and for different nanocapsules under investigation. The low absorbance change of DPPH in the presence of curcumin suggests a strong scavenging ability of curcumin which is attributed to the donation of H from the  $\beta$ -diketone group of curcumin to DPPH<sup>45</sup>. DPPH radical scavenging mechanism is depicted in **Scheme 3**<sup>46</sup>. However, the change in absorbance increased 17 fold for the largest nanocapsules under study compared to the same amount of curcumin. This low value is not surprising, as curcumin content in these microcapsules (NC1) is about 6 or 7 %, therefore, a 15 fold decrease in DPPH scavenging

activity is expected as per percentage of availability of curcumin over total weight of the nanocapsules. The further 2 fold decreases could be due to decrease in H-donation ability from the  $\beta$ -diketone group of curcumin to DPPH because of interaction between PAH/silica nanoparticles and curcumin. When the DPPH scavenging activity was compared with other smaller sized nanocapsules, the scavenging activity decreased exponentially with the size of the capsules, as shown in plot of  $1/\Delta A$  vs.  $R_h$  in **Figure 9b**. Although based on weight percentage, it was expected to have similar scavenging activity for three other smaller size capsules, which is about 2 fold lower than that of NC1; the exponential reduction indicates that not only the weight percentage of curcumin in the nanocapsules plays a role, but also the availability of  $\beta$ -diketone group of curcumin for H-donation is important. As the size of the nanocapsules are larger, more curcumin per surface area of the nanocapsules are exposed outside for scavenging activity compared to small size nanocapsules where a substantial percentage of curcumin are buried/encapsulated inside the capsules without exposing themselves for scavenging activity.

#### 4. Conclusion

In summary, the interaction of silica nanoparticles with CU/PAH/dipotassium phosphate aggregates to produce spherical nanocapsules of sizes ranging between 100 and 1000 nm. The size of the capsule is controlled by the concentration of dipotassium phosphate where the plot of the hydrodynamic radius with different salt concentrations has showed an excellent linear relationship. Silica nanoparticles are concentrated at the peripheries whereas curcumin is distributed all over the capsule. The high value of the binding constant ( $K=1.44 \times 10^4 \text{ M}^{-1}$ ) for CU and PAH proves the strong interaction between these constructs. The nanocapsules are negatively charged. The percentage of CU for the largest NCs is 7% while its 4% for smaller capsules. In the capsule, CU is found in its enol form. The delivery of CU from the NCs is

favoured under basic conditions. Moreover, the drug release profile fits the Higuchi model. The DPPH scavenging activity of CU is decreased in the capsule. The reduction in the scavenging activity is related to the percentage by weight of CU in the capsule and the availability of the  $\beta$ -diketone group for H-donation. Thus, larger sized nanocapsules have more curcumin per surface area of the nanocapsules, which are exposed outside for scavenging activity compared to small sized nanocapsules where a substantial percentage of curcumin are buried/encapsulated inside the capsules without exposing themselves for scavenging activity.

### Acknowledgement

We appreciate the help of Tina Gulin (for TGA) and Didem Sen Karaman (for TGA) during our measurements. Financial support provided by Lebanese National Council of Scientific Research (NCSR), Lebanon and American University of Beirut, Lebanon through URB and Long-term development grants (DP) as well as Kamal A. Shair Central Research Laboratory (KAS CRSL) facilities to carry out this work is greatly acknowledged.

### Reference

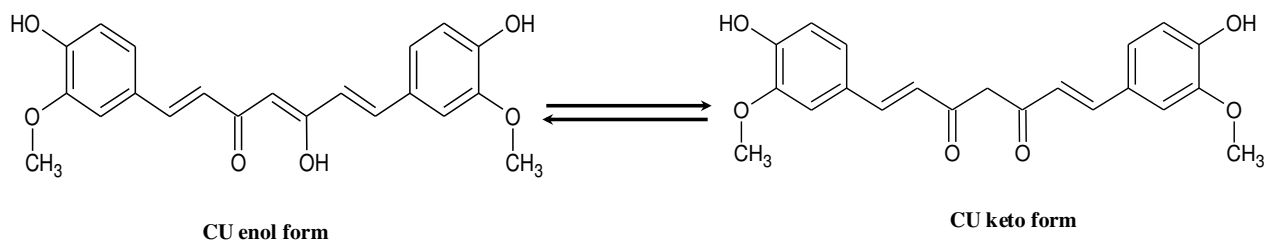
1. H. C. Zeng, *J. Mater. Chem.*, 2006, **16**, 649.
2. R. K. Rana, V. S. Murthy, J. Yu and M. S. Wong, *Adv. Mater.*, 2005, **17**, 1145.
3. G. C. Kini, S. L. Biswal, and M. S. Wong, Non-Layer-by-Layer Assembly and Encapsulation Uses of Nanoparticle-Shelled Hollow Spheres, In *Modern Techniques for Nano-and Microreactors/-reactions*, Springer Berlin Heidelberg, 2010, 89-114
4. V. S. Murthy, R. K. Rana and M. S. Wong, *J. Phys. Chem. B*, 2006, **110**, 25619.
5. G. C. Kini, J. Lai, M. S. Wong and S. L. Biswal, *Langmuir*, 2010, **26**, 6650.
6. J. Yu, V. S. Murthy, R. K. Rana and M. S. Wong, *Chem. Comm.*, 2006, **10**, 1097.
7. H. G. Bagaria, M. R. Dean, C. A. Nichol and M. S. Wong, *J. Chem. Educ.*, 2011, **88**, 609.

8. H. G. Bagaria and M. S. Wong, *J. Mater. Chem.*, 2011, **21**, 9454.
9. L. Nardo, A. Andreoni, M. Bondani, M. Måsson and H. Hjorth Tønnesen, *J. Photochem. Photobiol. B*, 2009, **97**, 77.
10. S. Shishodia, M. M. Chaturvedi and B. B. Aggarwal, *Curr. Probl. Can.*, 2007, **31**, 243.
11. D. Patra and C. Barakat, *Spectrochimica Acta Part A*, 2011, **79**, 1823.
12. R.N. Chopra, I.C. Chopra, K.L. Honada and L.D. Kapur, *Indigenous Drugs of India*, second ed., Duhr, Calcutta, 1958.
13. A. Krishnamoorthy, *The Wealth of India: A Dictionary of Indian Raw Materials and Industrial Products*, CSIR, New Delhi, 1950, **2**, 402.
14. J. T. Mague, W.L. Alworth and F.L. Payton, *Acta Cryst. C* 2004, **60**, 608.
15. A. Khafif, S.P. Schantz, T.C. Chou, D. Edelstein and P.G. Sacks, *Carcinogenesis*, 1998, **19**, 419.
16. M.T. Huang, R.C. Smart, C.Q. Wong and A.H. Conney, *Cancer Res.*, 1988, **48**, 5941.
17. J. Woo, Y. Kim, Y. Choi, D. Kim, K. Lee, J.H. Bae, D.S. Chang, Y.J. Jeong, Y.H. Lee, J. Park and T.K. Kwon, *Carcinogenesis* 2003, **24**, 1199.
18. M. J. Van Erk, E. Teuling, Y. C. M. Staal, S. Huybers, P. J. van Bladeren, J. M. M. J. G. Aarts and B. van Ommen, *J. Carcinogen.* 2004, **3**, 1.
19. R. C. Srimal and B. N. Dhawan, *J. Pharm. Pharmacol.* 1973, **25**, 447.
20. Y. Kiso, Y. Suzuki, N. Watanabe, Y. Oshima and H. Hikino, *Planta Med.*, 1983, **49**, 185.
21. S.D. Deodhar, R. Sethi and R.C. Srimal, *Indian J. Med. Res.*, 1980, **71**, 632.
22. W. C. Jordan and C. R. Drew, *J. Natl. Med. Assoc.*, 1996, **88**, 333.
23. R. De, P. Kundu, S. Swarnakar, T. Ramamurthy, A. Chowdhury, G.B. Nair and A. K. Mukhopadhyay. *Antimicrob. Agents Chemother.*, 2009, **53**, 1592.

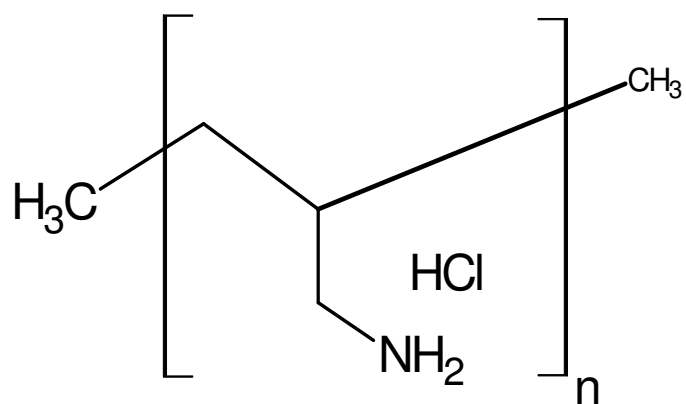
24. Y. Wang, Z. Lu, H. Wu and F. Lv, *Int. J. Food Microbiol.*, 2009, **136**, 71.
25. R. Srivastava, M. Dikshit, R.C. Srimal and B.N. Dhawan, *Thromb. Res.*, 1985, **40**, 413.
26. F. Yang, G. P. Lim, A. N. Begum, O. J. Ubeda, M. R. Simmons, S. S. Ambegaokar, P. Chen, R. Kaye, C. G. Glabe, S. A. Frautschy and G. M. Cole, *J. Biol. Chem.* 2004, **280**, 5892.
27. M. E. Egan, M. Pearson, S. A. Weiner, V. Rajendran, D. Rubin, J. Glochner-Pagel, S. Canney, K. Du, G. L. Lukacs and M. F. Caplan, *Science*, 2004, **304**, 600.
28. A. L. Cheng, C. H. Hsu, J. K. Lin, M. M. Hsu, Y. F. Ho, T. S. Shen, J. Y. Ko, J. T. Lin, B. R. Lin, W. Ming-Shiang, H. S. Yu, S. H. Jee, G. S. Chen, T. M. Chen, C. A. Chen, M. K. Lai, Y. S. Pu, M. H. Pan, Y. J. Wang, C. C. Tsai and C. Y. Hsieh, *Anticancer Res.* 2001, **21**, 2895.
29. B. Wahlstrom and G. Blenow, *Pharmacol. Toxicol.*, 1978, **43**, 86.
30. R. K. Basniwal, H. S. Buttar, V. K. Jain and N. Jain, *J. Agricul. Food Chem.*, 2011, **59**, 2056.
31. P. Anand, H. B. Nair, B. Sung, A. B. Kunnumakkara, V. R. Yadav, R. R. Tekmal and B. B. Aggarwal, *Biochem. Pharmacol.*, 2010, **79**, 330.
32. R.K. Das, N. Kasoju and U. Bora, *Nanomedicine*, 2010, **6**, 153.
33. D. Wang, M.S. Veena, K. Stevenson, C. Tang, B. Ho, J.D. Suh, V.M. Duarte, K.F. Faull, K. Mehta, E.S. Srivatsan and M.B. Wang, *Clin. Cancer Res.*, 2008, **14**, 6228.
34. N.W. Clifford, K.S. Iyer and C.L. Raston, *J. Mat. Chem.* 2008, **18**, 162.
35. S. Bisht, M. Mizuma, G. Feldmann, N. A. Ottenhof, S. -M. Hong, D. Pamanik, V. Chenna, C. Karikari, R. Sharma, M. G. Goggins, M. A. Rudek, R. Ravi, A. Maitra and A. Maitra, *Mol. Cancer Ther.* 2010, **9**, 2255.

36. S. Bisht, G. Feldmann, S. Soni, R. Ravi, C. Karikar, A. Maitra and A. Maitra, *J. Nanobiotechnol.* 2007, **5**, 3.
37. M. M. Yallapu, B. K. Gupta, M. Jaggi, S. C. Chauhan, *J. Colloid Interface Sci.*, 2010, **351**, 19.
38. R. K. Bhawana, H.S. Basniwal, V.K. Buttar and N. Jain, *J. Agric. Food Chem.* 2011, **59**, 2056..
39. K. Maiti, K. Mukherjee, A. Gantait, B. P. Saha and P. K. Mukherjee, *Int. J. Pharm.*, 2007, **330**, 155.
40. D. Patra and F. Sleem, *Anal. Chim. Acta*, 2013, **795**, 60.
41. D. Patra, A. J. Amali and R. K. Rana, *J. Mater. Chem.*, 2009, **19**, 4017.
42. A.J. Amali, N.H. Awwad, R.K. Rana and D. Patra, *Anal. Chim. Acta* 2011, **708**, 75.
43. P. Zhang, X. Song, W. Tong and C. Gao, *Macromolecu. Biosci.*, 2014, **14**, 1495.
44. M. Mauslmani and D. Patra, *RSC Adv.*, 2014, **4**, 8316.
45. S. V. Jovanovic, S. Steenken, C. W. Boone and M. G. Simic, *J. Am. Chem. Soc.* 1999, **121**, 9677.
46. B. Ozcelik, J. H. Lee and D. B. Min, *J. Food Sci.*, 2003, **68**, 487.
47. K. A. Connors, *Binding Constants. The measurements of molecular complex stability.* Wiley, New York, 1987.
48. C. Barakat and D. Patra, *Luminescence*, 2013, **28**, 179.
49. C. A. Mirkin, R. L. Letsinger, R. C. Mucic and J. J. Storhoff, *Nature*, 1996, **382**, 607.
50. R. F. Pasternack, C. Bustamante, P. J. Collings, A. Giannetto and E. J. Gibbs, *J. Amer. Chem. Soc.*, 1993, **115**, 5393.

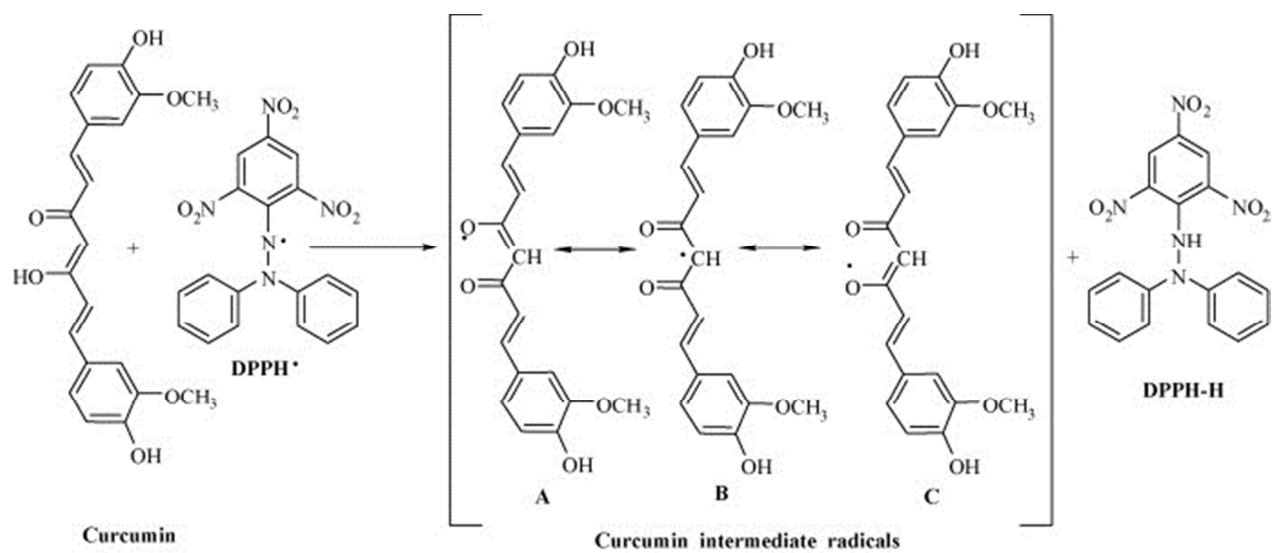
51. C. Xie, F. G. Xu, X. Y. Huang, C. Q. Dong and J. C. Ren, *J. Amer. Chem. Soc.*, 2009, **131**, 12763.
52. T. M. Kolev, E. A. Velcheva, B. A. Stamboliyska and M. Spitteller, *Int. J. Quant. Chem.*, 2005, **102**, 1069.
53. T. Higuchi, *J. Pharm. Sci.*, 1963, **52**, 1145.



**Scheme 1:** Chemical structures of curcumin tautomers.



**Scheme 2:** Chemical structure of poly (allylamine hydrochloride) (PAH).



**Scheme 3:** The proposed 2,2-diphenyl-1-picrylhydrazyl (DPPH) scavenging mechanism of curcumin<sup>45</sup>.

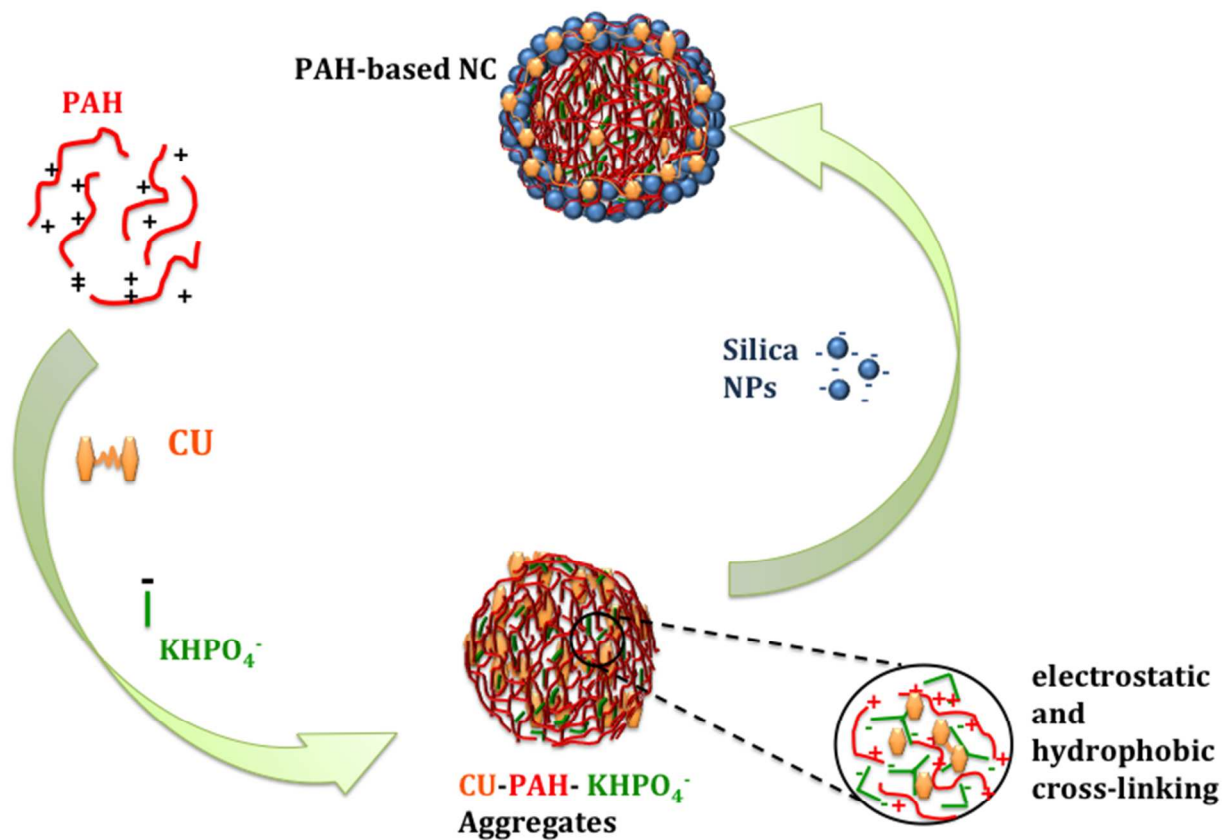


**Figure 1:** Illustration of CU interacting with PAH, dipotassium phosphate and SiO<sub>2</sub> NPs to form NCs.

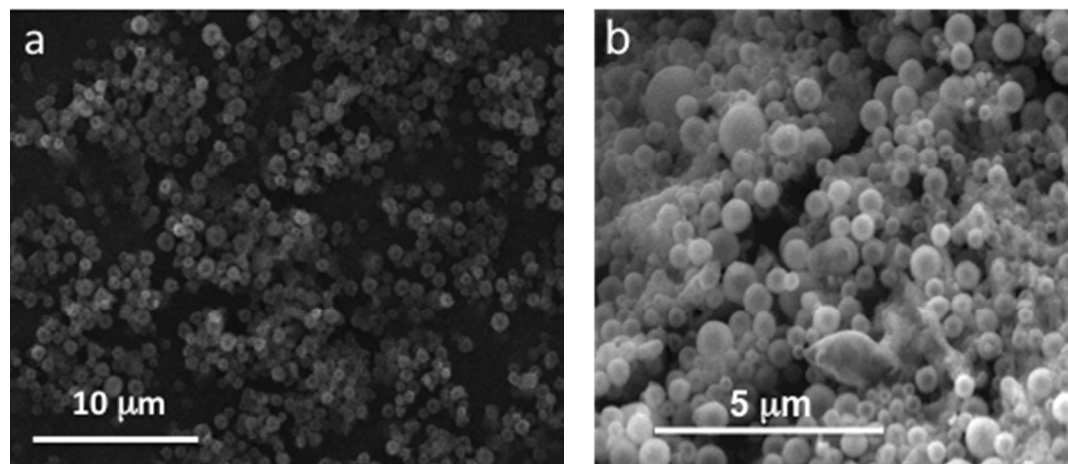


**Figure 2:** SEM images of NCs; (a) 10 μm resolution (b) 5 μm resolution.

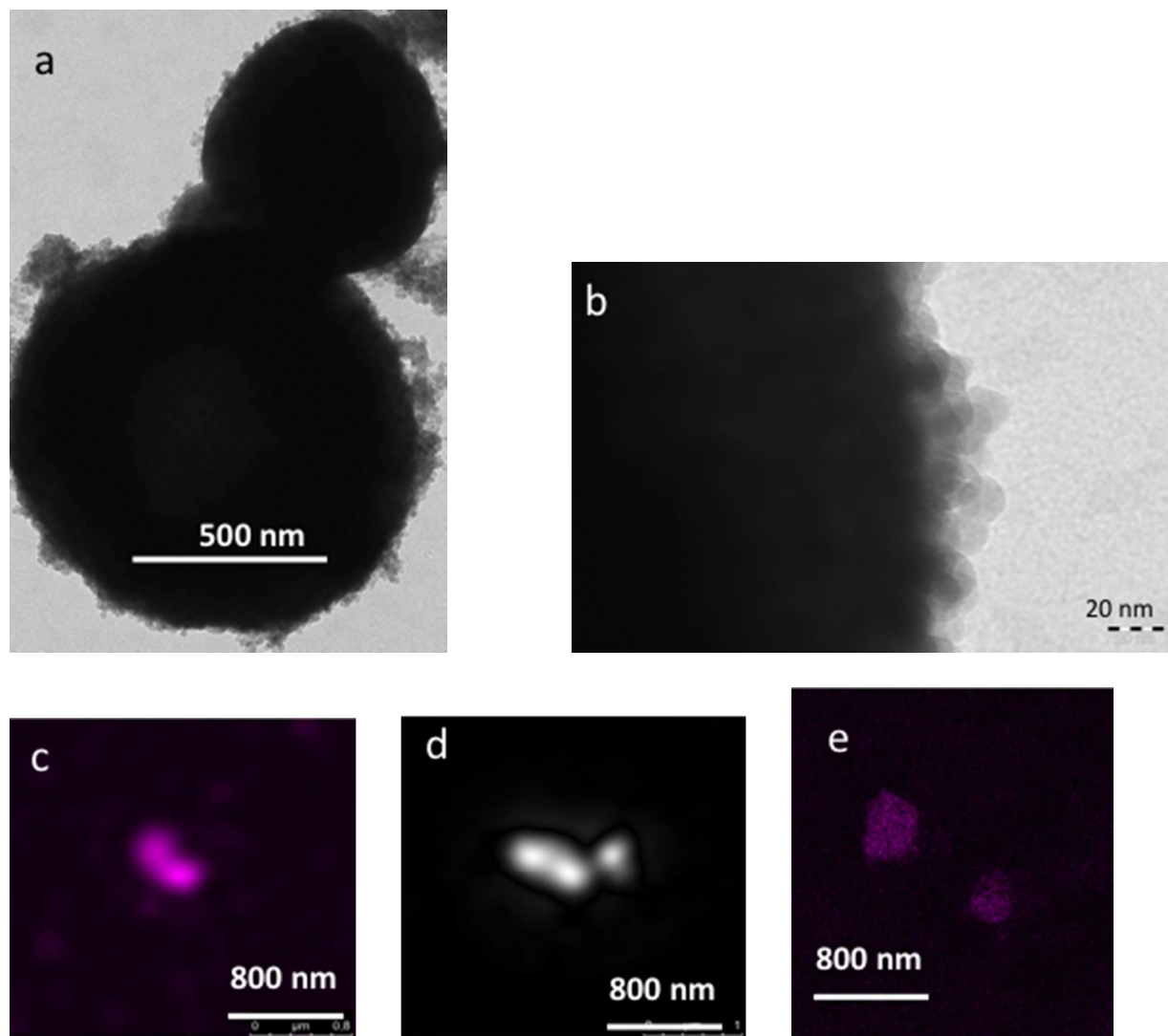


**Figure 3:** (a, b) TEM image of Nanocapsules, NC1, scale bar is 500 nm for (a) and 20 nm for (b); (c, e) Confocal fluorescence microscope images of curcumin encapsulated microcapsules; (d) 3D orientation of the image of aggregated NCs in (c).

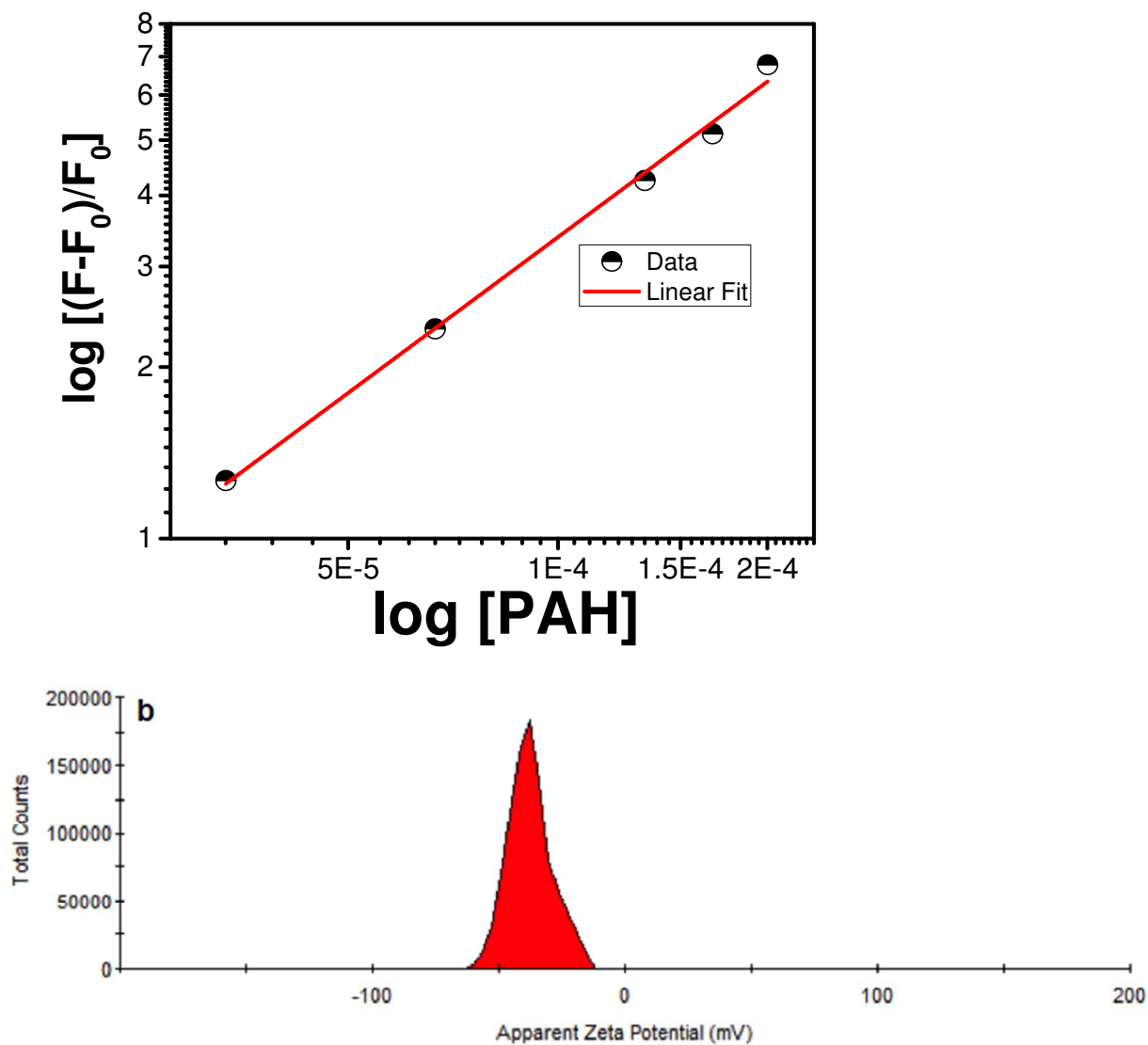


**Figure 4:** (a) Plot of  $[\text{PAH}]$  vs.  $(F-F_0)/F_0$ . The concentration of curcumin was fixed at  $9.0 \mu\text{M}$  whereas the concentration of PAH ranged between 0 and 3 mg/ml.  $F$  and  $F_0$  are the fluorescence intensities of CU in the presence and absence of PAH respectively. The excitation wavelength was 355 nm and the emission wavelength was 440 nm. (b) Apparent zeta potential distribution of nanocapsules.

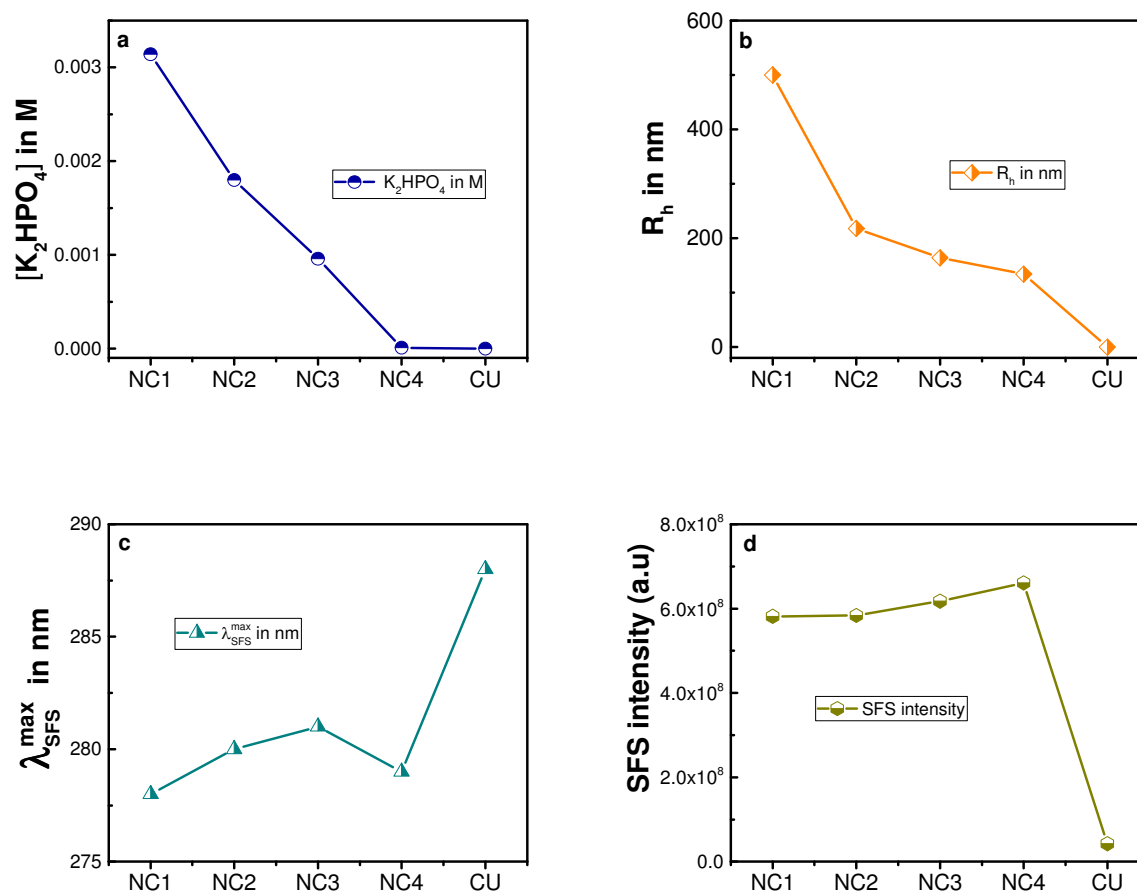


**Figure 5:** Characterization of different Nanocapsules based on change in salt concentration (a), hydrodynamic radius (b) and Resonance Rayleigh Scattering measured in synchronous fluorescence spectroscopic (SFS) mode with a  $\Delta\lambda = 0$  nm, thus,  $\lambda_{\text{SFS}}$  (max) and SFS intensity correspond to RRS maximum and RRS intensity respectively. NC1, NC2, NC3 and NC4 represent nanocapsules (NCs) with  $R_h$  values of 500 nm, 218 nm, 164 nm and 133 nm, respectively. CU: curcumin in double distilled water.

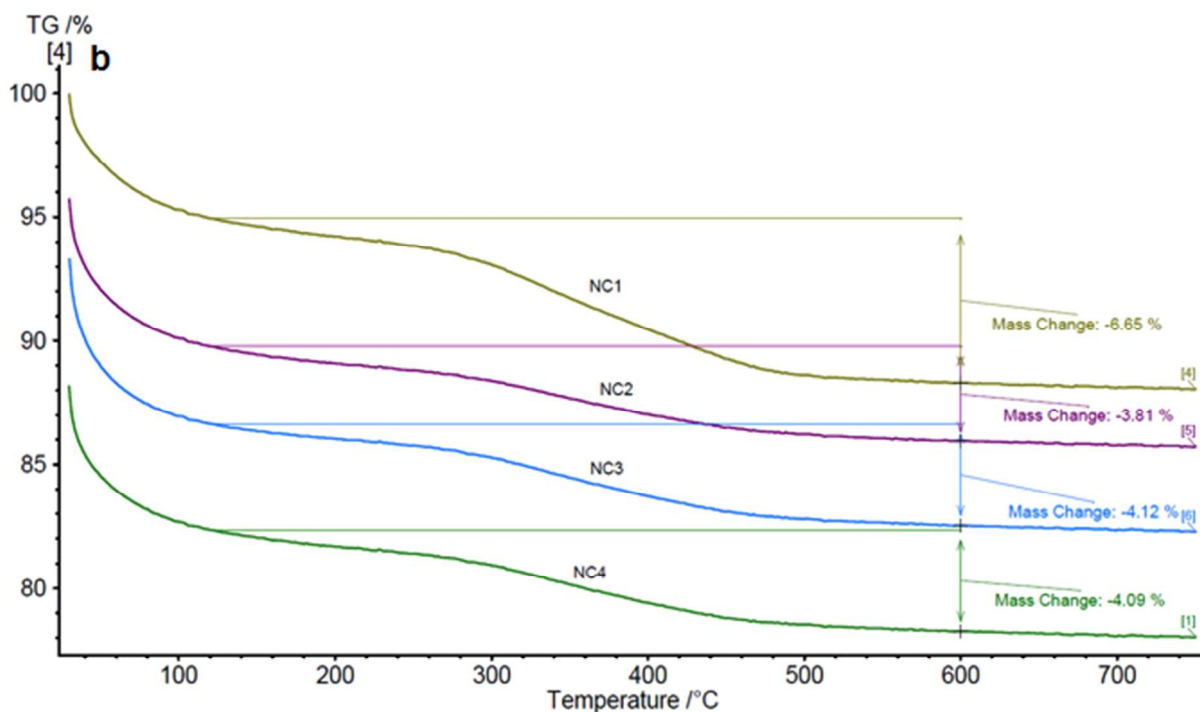
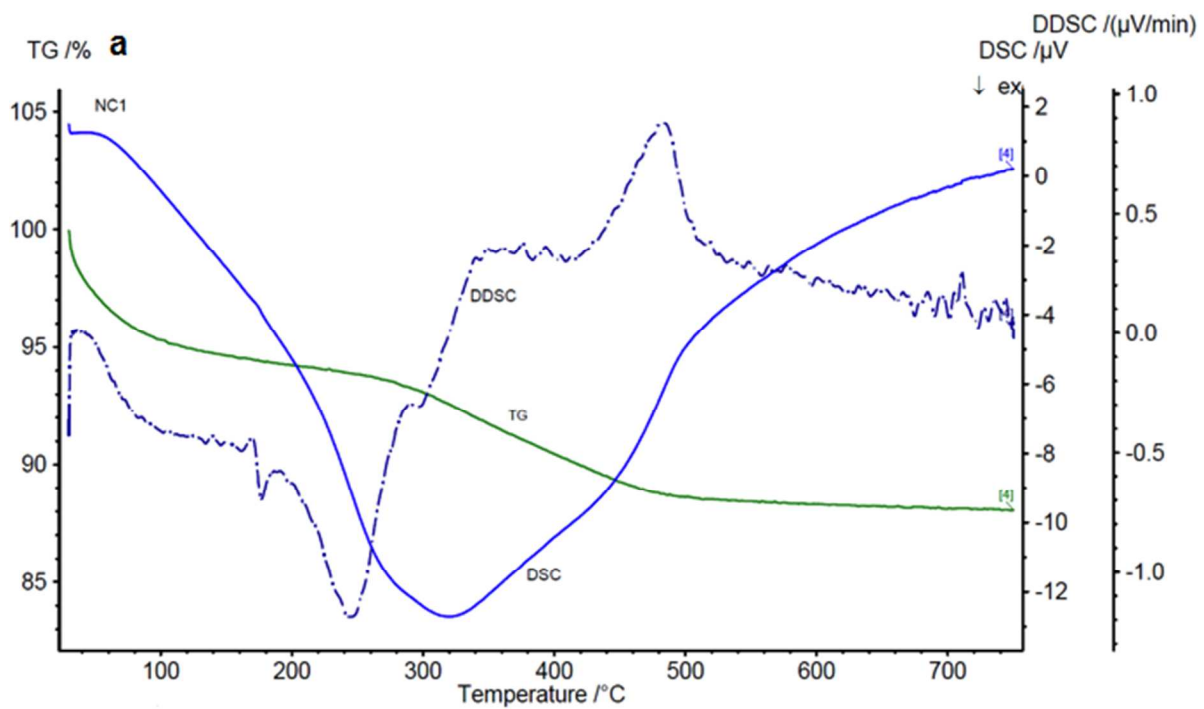


**Figure 6:** (a) Thermogravimetric analysis of nanocapsule. TG: Thermogravimetric; DSC: Differential scanning calorimetry; DDSC: Derivative of differential scanning calorimetry. (b) Comparison of thermogravimetric analysis of different nanocapsules. NC1, NC2, NC3 and NC4 represent nanocapsules (NCs) with  $R_h$  values of 500 nm, 218 nm, 164 nm and 133 nm, respectively.

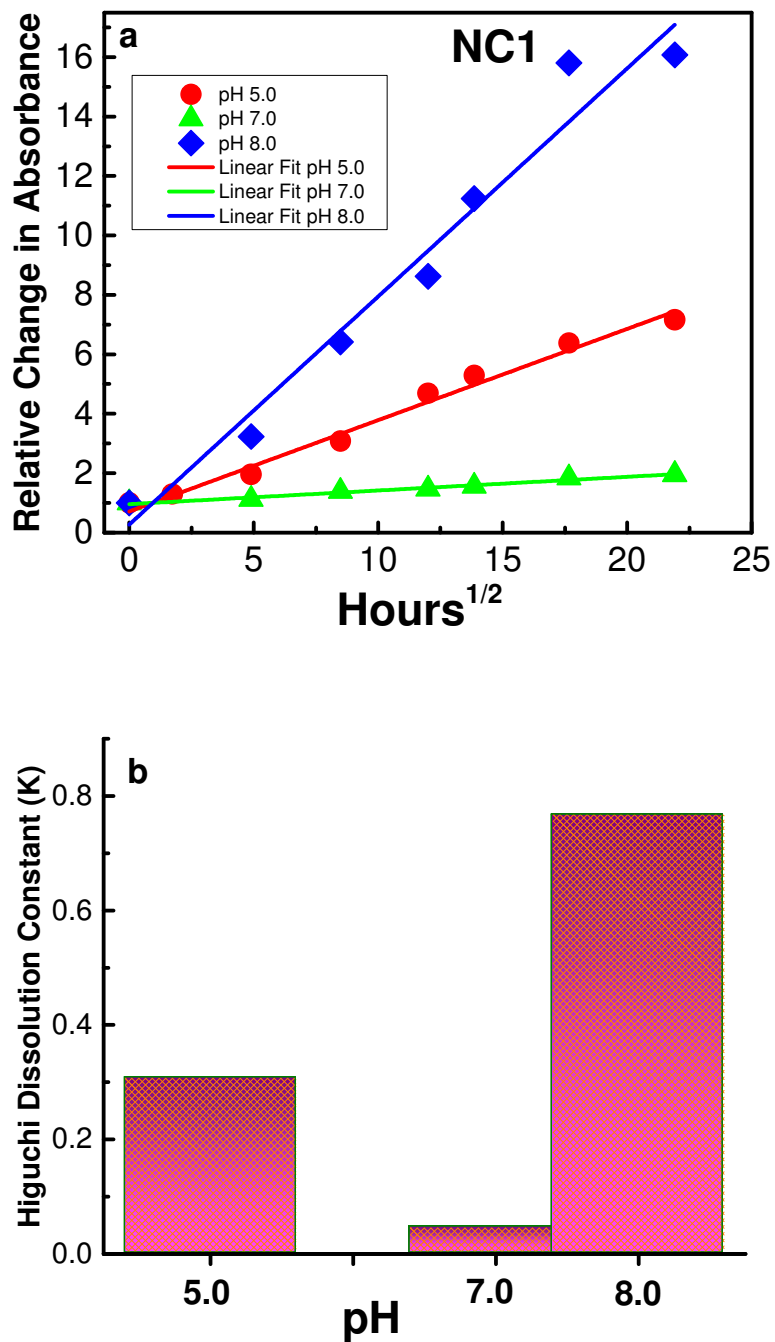


**Figure 7:** (a) Release of curcumin measured in absorbance scale from NC1 in different pH condition. Data were fitted with Higuchi model<sup>53</sup> for drug release. (b) Comparison of Higuchi dissolution constant in different pH.

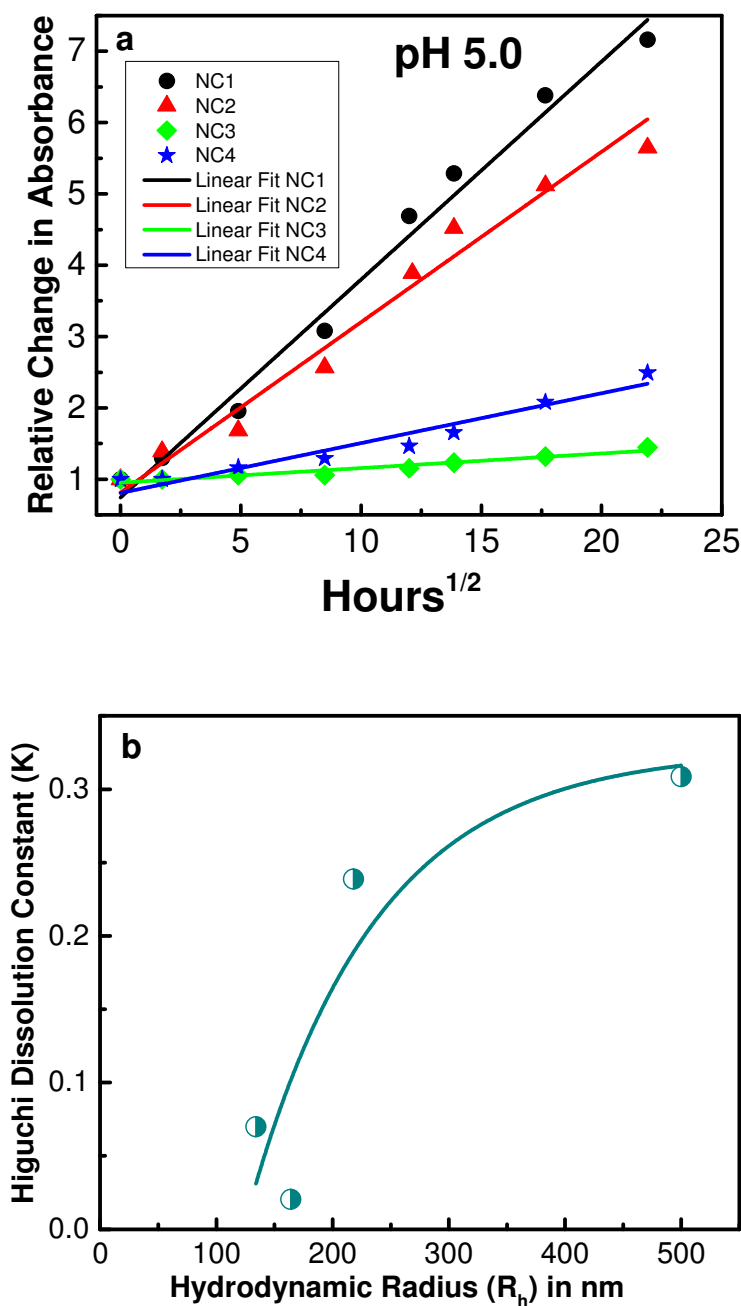


**Figure 8:** (a) Release of curcumin measured in absorbance scale from different nanocapsules in pH 5.0. Data were fitted with Higuchi model<sup>53</sup> for drug release. (b) Higuchi dissolution constant ( $K_H$ ) versus particle size. NC1, NC2, NC3 and NC4 represent nanocapsules (NCs) with  $R_h$  values of 500 nm, 218 nm, 164 nm and 133 nm, respectively.

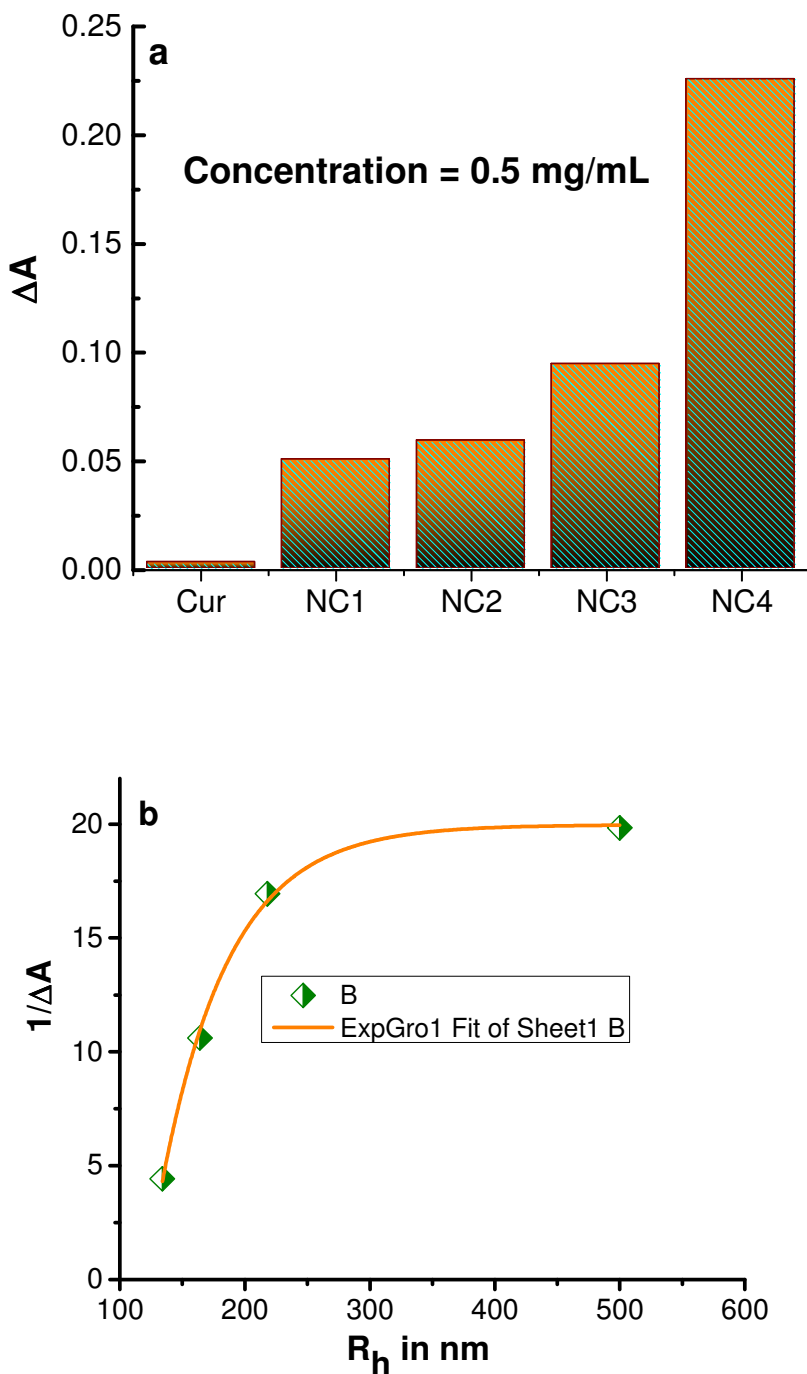


**Figure 9:** (a) Change in DPPH absorption at 520 nm in the presence of curcumin and nanocapsules of different sizes in de-ionized water at room temperature. The concentration of curcumin and nanocapsules was fixed at 0.5 mg/ml and that of DPPH at 100  $\mu$ M. (b)  $1/\Delta A$  of DPPH at 520 nm vs.  $R_h$  of nanocapsules indicating exponential increase in DDPH scavenging activity of CU. NC1, NC2, NC3 and NC4 represent nanocapsules (NCs) with  $R_h$  values of 500 nm, 218 nm, 164 nm and 133 nm, respectively. CU: curcumin.